1

Introduction

Immediately following the Big Bang, matter in the Universe was distributed very uniformly. However, gravitational interaction caused minor overdensities that slowly attract surrounding matter to further increase in density. For the first 380,000 years, the baryonic matter in the Universe was in an ionized state due to its high temperature. This caused matter to be tightly coupled to photons, which counteract the gravitational clustering of matter. Only dark matter, which does not couple to photons, was able to immediately initiate gravitational collapse. As the Universe expanded and cooled down, baryonic matter started to recombine into neutral atoms, causing it to decouple from photons. An imprint of the density of baryonic matter at this time remains visible as the Cosmic Microwave Background (CMB, Planck Collaboration 2020). As matter gravitationally collapses, it forms denser "walls" of matter encompassing large voids in the Universe. Where these walls meet, they in turn collapse into narrow filaments. Finally, at the intersections of filaments, we see the formation of very dense nodes. This distribution of matter in the Universe is referred to as the "Cosmic Web". Within the Cosmic Web, the first stars and galaxies were able to form. At the nodes of the Cosmic Web, these galaxies grouped together to form large clusters of galaxies (see Figure 1.1), which are the most massive gravitationally bound structures in the Universe with masses on the order of $10^{14} - 10^{15}$ solar masses (e.g., Peebles & Yu 1970; Press & Schechter 1974).

Galaxies and galaxy clusters are one of the main topics of current astronomical research. These objects undergo major changes from their initial formation to the present day, experience strong interactions with other galaxies and galaxy clusters, and feature complex interactions between their different components. This leaves major questions as to how exactly these objects form and evolve throughout cosmic time.

1.1 Galaxy clusters

The galaxy clusters we observe today have formed hierarchically through the mergers of smaller galaxy clusters to create more massive galaxy clusters. Merger events are some of the most energetic events in the Universe (e.g., Markevitch et al. 1999),

Figure 1.1: The galaxy cluster eMACS J1823.1+7822 as captured by the Hubble Space Telescope. Image credit: ESA/Hubble & NASA, H. Ebeling

and have considerable impact on the individual components of the galaxy cluster. As such, we typically classify galaxy clusters based on their dynamical state: relaxed clusters and recent mergers.

Unlike what their name suggests, galaxies comprise only about 10% of the total baryonic mass in galaxy clusters (e.g. Chiu et al. 2018). The vast majority of the mass is part of the extremely hot ionized gas known as the intracluster medium (ICM). Due to its temperature of around 10^{7-8} K, the ICM produces strong thermal bremsstrahlung, which is observed as bright radiation in the X-ray regime (e.g., Gursky et al. 1971; Forman et al. 1972), as shown in Figure 1.2. The emission of this radiation comes at the cost of the internal energy of the ICM, resulting in a cooling effect. As the ICM cools down in its central regions, where the cooling effect is the strongest, it is drawn to the center of the cluster by gravity. There, it compresses in order to retain the internal pressure required to support its own weight. This in practice means that the emission of X-ray radiation causes the ICM to sink down the gravitational well in what is known as a *cooling flow* (e.g., Fabian 1994). At the core of the cluster, we commonly find a massive central galaxy which dominates the local region and can be easily identified as it is often the brightest cluster galaxy (BCG). When the cooling flow reaches the center of the cluster, it accretes onto the BCG. In this central galaxy, the cooled ICM gives rise to star-formation and fuels the supermassive black hole (SMBH) located in the core of the galaxy.

Although being a physically sound model, a number of observations indicate that the previously described cooling process does not actually take place as described. First of all, by comparing the X-ray brightness of the ICM with the internal energy of this medium, one can predict how long it takes for the ICM to fully cool down. For relaxed clusters, this is typically less than the Hubble time within approximately 100 kpc, and further decreases to less than a Gyr within approximately 10 kpc (Voigt & Fabian 2004). Based on this estimate, the ICM is expected to cool down on such short time scales that it should no longer remain present in modern-day galaxy clusters.

Additionally, the X-ray luminosity of a typical galaxy cluster suggests that the cooling flow should deposit up to 1000 $M_\odot$ of ICM per year onto the central BCG (e.g., Edge et al. 1992). However, the high star-formation rates which would be enabled by such a cooling flow are in general not observed (e.g., Fabian et al. 1982; McNamara & O'Connell 1989; Kaastra et al. 2001; Peterson et al. 2003; Peterson & Fabian 2006). This further suggests that the predicted cooling flows are prevented by a process which compensates for the ICM's radiative cooling.

We now understand that the SMBH in the central BCG plays a key role in the galaxy cluster. As the SMBH is fed by the surrounding cold gas, part of the energy involved in this process is released back into the environment, resulting in a strong feedback process. This feedback re-energizes the ICM, thereby preventing the ICM from rapidly cooling down and forming stars (e.g., McNamara & Nulsen 2007; Fabian 2012; Gitti et al. 2012a).

In addition to their galactic overdensity and the bright X-ray emission produced by their ICM, galaxy clusters can be recognized through the interaction of their hot ICM with the CMB, known as the Sunyaev-Zel'dovich (SZ, Sunyaev & Zeldovich

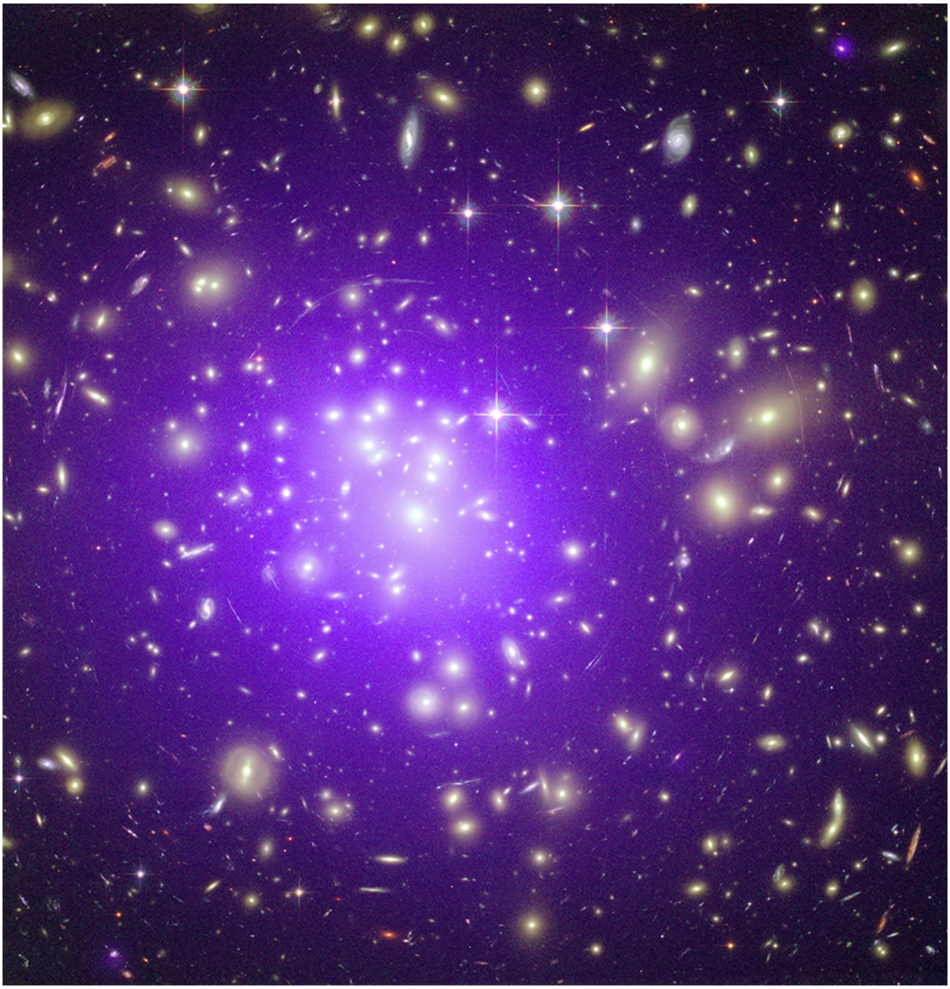

Figure 1.2: Composite image of the Abell 1689 galaxy cluster showing both the galactic population of the cluster (yellow) as well as the intracluster medium (purple). Image credit: X-ray: NASA/CXC/MIT/Peng et al. (2009); Optical: NASA/STScI.

1970) effect. As low-energy CMB photons collide with the high-energy cosmic rays of the ICM, they are scattered up to higher energies. At the typical wavelengths at which the CMB is observed, this leaves behind a "shadow" created by the galaxy cluster, allowing these clusters to be detected up to the proto-cluster regime (e.g., Overzier 2016). Unlike X-ray observations, which are most sensitive to nearby galaxy clusters, the shadow in the CMB created by the SZ effect is largely redshift-independent. This makes SZ observations very valuable for the detection of distant galaxy clusters.

1.2 Active galactic nuclei

At the core of practically all galaxies, a SMBH can be found (e.g., Kormendy & Gebhardt 2001; Merritt & Farrarese 2001; Häring & Rix 2004). These SMBHs can be fed with cold gas from within the galaxy. This creates what is known as an active galactic nucleus (AGN, e.g., Fabian 1999). As the gas is captured by the gravitational pull of the black hole, the combination of its angular momentum and the black hole's spin compresses it into an accretion disk surrounding the black hole. The infalling material releases a large fraction (up to $\sim$10%) of its rest-mass energy in this process, which makes AGNs some of the most luminous objects in the Universe.

AGNs have been empirically classified into several categories, depending on their observed features. These features probe different physical properties. In addition, the angle with which we observe the black hole and its accretion disk can play a critical role in obscuring and revealing particular components (e.g., Antonuci 1993; Urry & Padovani 1995; Netzer 2015).

For some AGN we have a direct view of the extremely hot and high-velocity gas of the accretion disk near the black hole. In optical observations, such systems show high luminosities and broad emission lines, and are classified as Type 1 AGNs. On the contrary, if we are viewing the AGN from the side, the dusty torus obscures the inner region near the SMBH, causing us to only observe the slowly-moving gas towards the outer regions of the accretion disk. These systems show relatively narrow emission lines, and are classified as Type 2 AGNs (e.g., Khachikian & Weedman 1974).

Depending on the ratio between the radio flux and the optical flux, AGN can also be classified into the radio-loud of radio-quiet categories (Kellerman et al. 1989). Radio-loud AGNs feature jetted outflows, which are ejected from the inner region of the black hole along the spin axis of the black hole up to relativistic speeds. An example of this is shown in Figure 1.3. These jetted outflows can escape the host galaxy of the AGN and propagate into intergalactic space. Depending on the morphology of these outflows, these can be classified as either a type 1 or a type 2 within the Fanaroff-Riley scheme (Fanaroff & Riley 1974). A Fanaroff-Riley Type 1 (or FR-I) typically shows bright jets near the AGN, which slowly diffuse away as they propagate away from the core of the AGN. On the other hand, a Fanaroff-Riley Type 2 (or FR-II) source has jets which terminate in hot spots on opposite sides of the AGN, typically surrounded by radio lobes.

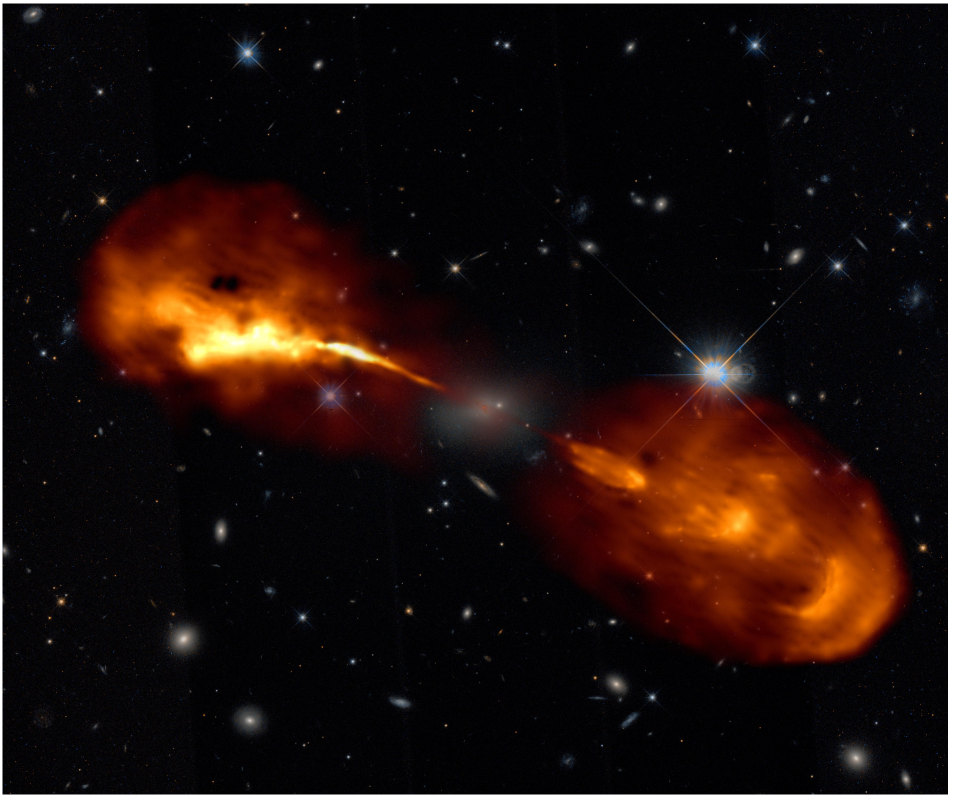

Figure 1.3: Composite image of Hercules A. The high-resolution 144 MHz radio image is shown in orange, and reveals two relativistic jets shooting away in opposite directions from the central supermassive black hole. Image credit: R. Timmerman/LOFAR, Hubble Space Telescope.

At the extremely luminous end, we find quasi-stellar objects (QSOs) or quasars, which can feature bolometric luminosities up to 10^{47} erg/s, and are most commonly found at relatively high redshifts of $z \approx 2$. Their brightness allows these objects to be detected at very large distances, making these objects valuable probes into the Early Universe.

1.3 Feedback

Many processes related to galaxies, stellar populations and compact objects result in feedback cycles. These cycles are critical to understand as they play a major role in the formation and evolution of many different types of objects. Two of the main forms of feedback in galaxies are supernovae feedback (e.g., Dale 2015) and AGN feedback (e.g., Brüggen & Kaiser 2002; McNamara & Nulsen 2007; Fabian 2012)

Supernovae feedback primarily occurs in star-forming regions. As gas clouds collapse under their self-gravity, stars of different masses form. The more massive stars have relatively short lifetimes and terminate as supernovae. These supernova explosions release large amounts of energy into the surrounding gas, produce shock waves and supply metals to their environment. This impacts the formation of new stars, by simultaneously disrupting gas which would have otherwise formed new stars and affecting the chemical composition of new stars.

Similarly, active galactic nuclei can also become part of the feedback cycle. An AGN has two main modes of feedback: radiative and mechanical feedback. Radiative feedback (also known as quasar-mode feedback, Croton et al. 2006) occurs due to the intense luminosity of the accretion disk. Due to the extreme temperature generated within the accretion disk, strong emission across practically all of the electromagnetic spectrum is released. This emission is so intense that its radiation pressure can expel the gas from the environment of the AGN and even large parts of the host galaxy. Not only can this restrict the inflow of new gas to the AGN, it can also limit the star-formation rate in the galaxy.

Secondly, mechanical (or radio-mode) feedback occurs as the matter falling towards the AGN is accelerated by the magnetic field of the black hole along its spin axis up to relativistic speeds, creating two jets of magnetized plasma travelling in opposite directions away from the AGN, as shown in Figure 1.4. Despite only constituting a fraction of the infalling matter, these jets can carry away a significant fraction of the available energy. In galaxy clusters, these typically escape the host galaxy and travel into the cluster environment. Here, they eventually slow down and end up producing large radio lobes (Bridle & Perley 1984). These radio lobes inflate against the external pressure of the ICM, producing bubbles or cavities within the ICM (e.g., Böhringer et al. 1993; Carilli et al. 1994). This way, the AGN is able to return energy to the cooling ICM, which initially fed the AGN, thereby preventing it from cooling down at its maximum rate. In turn, this reduces the star-formation rate of the central galaxies within the cluster. Unlike radiative feedback, which typically continues to grow in intensity as the AGN is fueled by more infalling matter, mechanical feedback is generally thought to level off at a

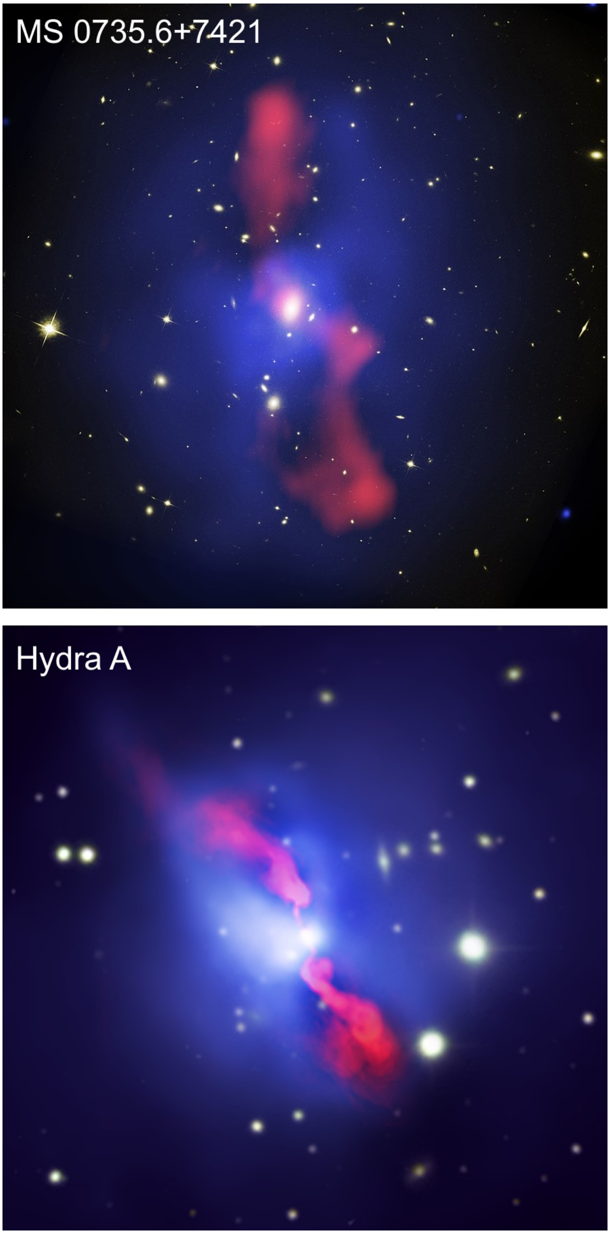

Figure 1.4: AGN feedback in the Hydra A and MS 0735.6+7421 galaxy clusters. The radio lobes, as observed at radio wavelengths, are shown in red. The ICM, observed at X-ray wavelengths, is shown in blue. Image credit for Hydra A: NASA/NSF/NRAO/CXC/VLA/Canada-France-Hawaii-Telescope/DSS/U.Waterloo/C.Kirkpatrick et al. Image credit for MS 0735.6+7421: NASA/ESA/CXC/STScl/NRAO/Univ. Waterloo/Ohio Univ./McNamara et al. (2009)

few percent of the Eddington rate (Russell et al. 2013), thereby allowing AGNs to produce feedback through both modes at different intensities. This provides a valuable opportunity to study not only the evolution of the ICM and the galaxies within the ICM, but also the growth of the SMBH powering the AGN.

Through the interaction between the radio lobes and the ICM, the average power injected by radio-mode AGN feedback into the cluster environment can be measured (e.g., Bîrzan et al. 2004; Rafferty et al. 2006; McNamara & Nulsen 2012). The total energy injected by the AGN can be estimated as the work required to inflate the radio lobes up to their current volume against the external pressure of the ICM plus the internal energy of the radio lobes. Assuming the radio lobes are composed of a relativistic gas, they will have an adiabatic index of $\gamma = 4/3$, and therefore we obtain

$$E_{\text{cav}} = E_{\text{internal}} + W = \frac{1}{\gamma - 1} pV + pV = 4pV. \tag{1.1}$$

By dividing this total energy output by the estimated age of the radio lobes, the average energy output of the AGN can be calculated. The age estimate is generally relatively uncertain and requires an assumption for the dynamics of the radio lobe. As the radio lobes are less dense than the surrounding ICM, they will buoyantly rise away from the center of the cluster. By assuming this dominated the motion or the radio lobe, the distance between the lobe and the AGN can be converted to an age estimate. An alternative is the assumption that the lobe travels at the speed of sound through the ICM, allowing for a similar conversion between distance and age. Typically, these estimates agree relatively well.

The feedback process is generally most reliably studied in relaxed clusters, as the cooling and heating processes can be assumed to be roughly in a steady state. We often observe the central ICM in a relaxed cluster to cool down, albeit not as rapidly as predicted. Nevertheless, this produces a cool-core region surrounding the BCG (e.g., Kaastra et al. 2001; Peterson et al. 2003). These cool cores generally do not survive merger events, making them an excellent indicator for relaxed galaxy clusters.

Current observations suggest that AGNs in galaxy clusters underwent a shift from operating primarily in quasar-mode in the Early Universe to operating primarily in radio-mode at the present day (Hlavacek-Larrondo et al. 2013). Currently, two scenarios would be consistent with this trend. Either the population of quasars increases in brightness towards higher redshifts, leading to sources being more likely to be detected at these higher redshifts, or there is an increase in the fraction of SMBHs which are active as quasars compared to the present day. The first scenario more naturally fits the data that AGNs produce more quasar-mode feedback towards high redshifts, but the lack of detection of quasar-mode feedback in some nearby clusters even with very deep X-ray observations leans more towards the second scenario. The evolution of AGN feedback over cosmic time would not only be a valuable probe to help constrain the environmental conditions of the AGNs in galaxy clusters, but it would also form a key constraint in models of the formation and evolution of galaxy clusters.

1.4 Observational instruments

Two parts of the electromagnetic spectrum are of particular interest for studies of active galactic nuclei and galaxy clusters: the radio and X-ray regimes. The immediate environment of the black hole is bright across practically the entire electromagnetic spectrum, including the radio and X-ray regimes. However, in addition to this, radio observations also provide an excellent view of the relativistic jets as they propagate into the cluster environment. The charged particles within these jets interact with the present magnetic field to produce synchrotron emission. This type of emission can generally be described using a power-law function within the radio regime, with the lower frequencies featuring higher intensities. Towards the high-frequency end of the radio spectrum, synchrotron emission typically cuts off due to aging. As the high-energy electrons produce high-frequency radio waves, they rapidly lose energy, causing these electrons to shift down to lower energies and therefore also lower frequencies.

Meanwhile, X-ray observations can be used to reveal the ICM. Due to its extremely high temperature, the ionized particles within the ICM produce thermal bremsstrahlung in the X-ray regime. Within the diffuse emission of the ICM, the cavities produced by AGN activity can also be detected. Furthermore, the spectrum of the X-ray emission can be used to constrain the physical properties of the ICM, such as the temperature and internal pressure.

1.4.1 Very Large Array

For the high-frequency radio observations used in this thesis, we rely on observations taken with the Very Large Array (VLA). This observatory was built near Socorro, New Mexico and is currently operated by the National Radio Astronomy Observatory (NRAO), Although commissioned in 1980, it has since been upgraded in 2012 to remain at the frontier of radio astronomy to date. This upgrade primarily focused on updating the receivers to improve the sensitivity and bandwidth coverage.

The VLA consists of 27 antennas with 25-meter fully steerable dishes divided over three arms in a Y-shape, as shown in Figure 1.5. To be able to perform both low- and high-resolution observations, these antennas are positioned on rails and can be placed in one of four configurations. The A-configuration, which is intended for the highest resolution imaging, the VLA has baseline lengths between 0.68 km and 36.4 km. In this configuration, the VLA offers an angular resolution of just over an arcsecond at 1.5 GHz (L band) and less than 0.05 arcseconds at 45 GHz (Q band). The array shrinks by roughly a factor of three each step from the A-configuration to the D-configuration, where it finally has baselines lengths between 35 m and 1.03 km. The VLA's set of 10 receivers offers a continuous frequency coverage from 1 to 50 GHz, with additional bands around 350 MHz (P band) and 74 MHz (4 band).

Figure 1.5: The Very Large Array in New Mexico, USA, shown in A-configuration. In the foreground, the antenna on position W08 is visible, with the Northern arm located in the background.

1.4.2 LOFAR

Towards the low-frequency radio regime, the LOw Frequency ARray (LOFAR, Van Haarlem et al. 2013) is the telescope offering the highest angular resolution. LOFAR contains two sets of antennas: the low-band antennas (LBA), which operate between 10 and 90 MHz, and the high-band antennas (HBA), which operate between 110 and 240 MHz. Instead of having movable dishes, LOFAR is divided up into stations which each contain multiple antennas. These antennas can be pointed to any position on the sky through electronics. After a direction has been selected, the difference in signal path length between all the individual dipoles of a station is calculated and corrected for. By summing up the signal accounting for this difference (also known as *beam-forming*), the signal from the selected direction is amplified, while signals from other directions are suppressed. As the pointing of the telescope is mainly performed digitally, LOFAR is able to observe multiple directions simultaneously, limited mainly by computational resources.

Although the core of LOFAR is located in the Netherlands, LOFAR also has stations located in other countries throughout Europe. This gives LOFAR a rare combination of very short baselines (down to 68 meters), and very long baselines (up to $\sim$1890 km). At the core, a cluster of six stations forms the “superterp” (see Figure 1.6). This is surrounded by the remaining core stations at slightly larger distances. For the core stations, the HBA tiles are split up into two separate substations. Further from the superterp, but still located in the Netherlands, LOFAR has additional remote stations, which use a combined station design. Finally, the international stations are larger versions of the Dutch stations, and are distributed across Europe.

Processing and analysing LOFAR observations provides several significant challenges. First, LOFAR observations are sensitive to large areas of the sky instanta-

Figure 1.6: The core of the LOw Frequency ARray (LOFAR), known as the "superterp". The LBA stations are the more "randomly" distributed wire dipoles, whereas the HBA stations are the gridded sets of dark grey boxes. Image credit: LOFAR.

neously. Therefore, it is difficult to isolate the emission from one radio source. For calibration and deconvolution, this requires imaging large fields, which is computationally expensive (Sweijen et al. 2022). Additionally, the data volumes which are produced by LOFAR observations are very challenging. A standard 8-hour observation produces around 4 terabytes of compressed data, or 14 terabytes of uncompressed data. This puts considerable hardware constraints on any computing cluster which is used for LOFAR data processing, and can make it difficult to work on large numbers of observations. Another challenge is that the remote and international stations operate on independent clocks due to their physical separation. This can introduce errors if these clocks drift relative to each other. To correct for this, careful calibration must take place. Fortunately, the LOFAR 2.0 upgrade is planned to place all remote stations on the same physical clock, largely resolving this problem for these stations. Finally, at the low radio frequencies where LOFAR observes, the Earth's ionosphere typically dominates the perturbation of the wavefront through the atmosphere (Intema et al. 2009; Mevius et al. 2016). Problematically, the ionosphere introduces phase errors which scale non-linearly with frequency. Generally, the first order effect is most significant. This is known to cause dispersive delays, which scale inversely with frequency. However, for the longest HBA baseline or generally in the LBA regime, the second order can not be neglected. Especially during high solar activity, the second order term can grow to be very significant. This can be recognized as Faraday rotation, and scales as inverse frequency squared (Sotomayor-Beltran et al. 2013). On top of that, these effects are strongly direction dependent, and can vary significantly across the field of view (Albert et al. 2020). Therefore, a single calibration solution which corrects for ionospheric perturbations across the entire field of view does not exist in general. This can be resolved by obtaining independent calibration solutions for multiple directions within the field and interpolating these. However, this is again a computationally demanding strategy.

All of the aforementioned challenges are intensified by the inclusion of LOFAR's international stations. These stations increase the angular resolution of LOFAR by a factor of around 20. With the HBA, this means that the angular resolution decreases from 6 arcseconds for the Dutch array to 0.3 arcseconds for the international array. To image the same field of view with the international stations requires roughly 400 times as many pixels. The increased angular resolution also results in decreased surface brightness sensitivity. After all, the same flux density will be distributed over far more individual resolution elements. Despite the added sensitivity gained by including the international stations, the resolution increase still causes a surface brightness sensitivity decrease of around a factor of 300. Additionally, the calibration models used to perform the calibration of the international stations must meet far higher fidelity standards than those used for the Dutch array. To calibrate the long baselines provided by the international stations, it is also required to have signal on corresponding angular scales. As it turns out, not many sources are simultaneously compact and bright at low frequencies. Finally, the phase errors due to the ionosphere increase with baseline length, which makes the international stations considerably more difficult to calibrate.

As wide-field imaging with the international stations is very computationally expensive, we are unable to perform calibration using the entire field of view, as we would do with the Dutch stations. Instead, the calibration strategy developed by Morabito et al. (2022) is based on imaging single targets, also known as "post stamp" imaging. By phasing up the core stations, averaging the data and applying a lower limit to the baseline lengths used during calibration, it is possible to reduce the interference from unrelated radio sources near the target of interest. The Long Baseline Calibrator Survey (LBCS, Jackson et al. 2016, 2022) provides a valuable catalog of bright and compact radio sources which can provide the signal on the long baselines to perform the calibration. Taking advantage of LOFAR's wide field, it is generally possible to find one of these calibrator sources within the field of view. This is particularly advantageous, as it allows for calibration solutions derived on the "in-field" calibrator to be applied to the target source without any temporal interpolation. Due to the non-linear nature of ionospheric phase errors, the fringe-fitting technique commonly used in VLBI is not applicable to LOFAR observations. Instead, we have to resort to a straight-forward phase solve in small bins of time and frequency, with only smoothing along the frequency axis to enhance the signal-to-noise ratio (Van Weeren et al. 2021).

The calibration of the Dutch part of the array is currently a solved problem (Van Weeren et al. 2016; Williams et al. 2016; de Gasperin et al. 2019), enabling the LOFAR Two-Metre Sky Survey (LoTSS, Shimwell et al. 2017, 2019). This survey aims to observe the entire Northern hemisphere using the Dutch LOFAR stations to provide a 144 MHz radio map with an angular resolution of 6 arcseconds. The current latest public data release (DR2, Shimwell et al. 2022) covers 27% of the Northern sky, reaching a depth of 83 µJy/beam. In addition to the images, a radio

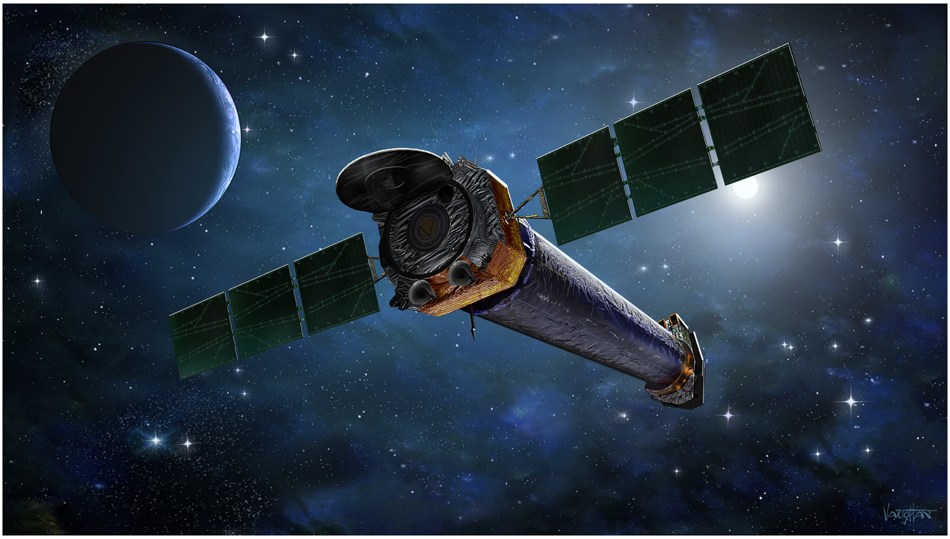

Figure 1.7: Artist impression of the Chandra X-ray Observatory. Image credit: NASA/CXC & J.Vaughan

source catalogue containing 4,396,228 sources was published.

1.4.3 Chandra

To study a critical component of galaxy clusters - the ICM - observations in the X-ray regime are required. As Earth's atmosphere is not transparent to X-ray photons, all X-ray observatories are space-based. The prime instrument for high angular resolution X-ray observations at the present time is the Chandra X-ray Observatory (Weisskopf et al. 2000), launched in 1999 by the Space Shuttle into a highly elliptical orbit (see Figure 1.7). This observatory offers a unique combination of angular and spectral resolution, which provide a uniquely detailed view of the X-ray sky. The Chandra X-ray Observatory contains multiple science instruments, such as the High Resolution Camera, the Low and High Energy Transmission Gratings and the Advanced Charged Couple Imaging Spectrometer (ACIS).

Of particular interest for galaxy cluster observations is the ACIS. By measuring both the direction and energy of incoming X-ray photons, the ten CCD chips of the ACIS provide a combination of imaging and spectroscopy with an angular resolution of only 0.5 arcseconds between 0.2 and 10 keV. Using this data, we are not only able to constrain the morphology of the ICM, but also its internal physical conditions such as the temperate and pressure. Additionally, the high angular resolution of the ACIS also allows the brightness from the AGN and the surrounding ICM to be disentangled.

1.5 Key questions

Active galactic nuclei and galaxy clusters have been active fields of research for multiple decades. Key questions have remained unanswered as to the formation and evolution of galaxy clusters, and the role of AGNs in that process. One of the key questions we are hoping to answer is how AGN feedback co-evolves with galaxy clusters. Initial indications suggest that AGN feedback may switch from a predominantly quasar-mode process to a more radio-mode process. Such an evolution in the way AGN feedback operates is critical to the interaction between the SMBH and its environment, and therefore also has a profound effect on the state of the ICM and star-formation in the cluster galaxies. Especially towards the Early Universe, observational constraints limit our understanding of the AGN feedback process.

Additionally, we need to understand how the mechanism of energy transfer from the relativistic jets of the AGN to the larger cluster environment. Fundamentally, this question is two-fold. First of all, it's not clear how the energy contained in the relativistic jets transfers to the ICM. Secondly, this energy also needs to be dissipated throughout the ICM. Radio-mode feedback is only emitted in two opposite directions in the cluster environment, but the ICM is distributed throughout the cluster.

Aside from the impact the AGN has on the large-scale environment, it is also valuable to understand the coupling to the environment of the host galaxy. For the host galaxy, the mode of feedback plays a significantly different role, with quasar-mode feedback having a much stronger effect. In addition, the host galaxy essentially regulates the flow of matter which feeds the AGN, and therefore also is key in understanding the duty cycle of the AGN.

Finally, the role of cluster mergers requires further investigation. Most research into AGN feedback gives preference to relaxed clusters due to practical considerations, but the effect of cluster mergers can not be neglected. Cluster mergers have a major impact on the dynamical state of the ICM as they can disrupt the cool core and introduce large-scale sloshing motions. Furthermore, the merging of the BCGs and eventually the central SMBHs plays a key role in their evolution, and therefore also the feedback cycle.

1.6 Thesis outline

The goal of this thesis is to study the study the operation of radio-mode feedback in galaxy clusters using radio and X-ray observations, with a particular focus on exploring the new parameter space available to us through the International LOFAR Telescope.

In **Chapter 2**, we study the mini halo and AGN of the Phoenix cluster at a redshift of $z = 0.597$. This cool-core cluster shows very high star-formation rates, indicating that the central AGN is failing to inhibit the cooling flow. Using multifrequency VLA observations between 1 and 12 GHz, we investigate the operation of the AGN in the center of the cluster as well as the origin of the mini halo. Based on the correlation between the X-ray and radio morphologies of the mini-halo, we conclude that the mini-halo is most likely formed through turbulent re-acceleration. Additionally, we find that time variability of the AGN likely results in an observed disconnection between the radio and X-ray properties of the system.

In **Chapter 3**, we use a combination of multifrequency VLA observations and ILT observations of Hercules A to study the origin of ring structures in one its radio lobes. Through spectral index measurements, we are able to constrain the electron population of the synchrotron-emitting plasma. This allows us to differentiate between the shock model and the inner-lobe model which both try to provide an explanation for the presence of the observed ring structures. Based on the spectral curvature trend in the rings, we find that the inner-lobe model is most consistent with our observations.

In **Chapter 4**, we present a sample of 14 cool-core galaxy clusters observed with the ILT, of which 8 observations including the international stations. With this sample, we check whether the low-frequency observations taken with LOFAR detect the complete volume of the radio lobes, as detected in X-ray observations. This way, we demonstrate that ILT observations are able to constrain this volume, which plays a key role in determining the energy output of the central AGN. In turn, this enables us to reach higher redshifts than before and measure the power of an AGN into the early Universe.

In **Chapter 5**, we report on the results of a pilot project where we observe a high redshift ($z > 0.6$) sample of galaxy clusters with the ILT. We test the method demonstrated in Chapter 4 on a high-redshift sample of targets for the first time to confirm that the method is feasible in the distant Universe, where X-ray observations alone can not reach the required sensitivity.

1.7 Future prospects

With the aid of a new generation of observatories such as the International LOFAR Telescope, the Square Kilometer Array (SKA), the ngVLA, XRISM, Athena and Euclid, as well as theoretical progress with cosmological simulations such as the EAGLE simulations (e.g., ARTEMIS and COLIBRI, Crain et al. 2015; Schaye et al. 2015; Font et al. 2020), further progress can be made to obtain the answers to the aforementioned questions. Large surveys of the sky which probe deeper than before provide valuable catalogs of galaxies, AGNs and galaxy clusters, and enable the population of these objects to be investigated in a statistically meaningful way. For example, the Euclid mission is expected to catalog $> 10^5$ galaxy clusters up to a redshift of $z = 2$ (Euclid Collaboration 2019), after which follow-up observations of these objects can be performed with next-generation instruments across a wide range of the electromagnetic spectrum.

Two of the main upcoming radio observatories are the SKA in the Southern Hemisphere and the ngVLA in the Northern Hemisphere. Both of these observatories will offer a revolutionary sensitivity to the radio sky together with an excellent angular resolution. This will not only enhance our understanding of bright and nearby radio sources, but also enable research on faint and distant radio sources which have not previously been studied. Similarly, the upcoming XRISM and Athena X-ray observatories are expected to provide an unparalleled combination of spectral resolution and sensitivity, which will enable groundbreaking new research on the physical properties of both AGNs and the ICM of galaxy clusters.

Of particular interest to this thesis is also the future upgrade of the International LOFAR Telescope to LOFAR 2.0 by ASTRON. This upgrade will improve our ability to perform high-resolution radio observations below 100 MHz, which will offer an unprecedented ability to study steep-spectrum radio emission. In time, this will provide us with a much more accurate understanding of the physics that govern AGN, galaxy clusters, and by extension our entire Universe.